Salt Enhances Calmodulin-Target Interaction

Ingemar André,* Tõnu Kesvatera,*† Bo Jönsson,‡ and Sara Linse*
*Department of Biophysical Chemistry, Lund University, Chemical Centre, Lund, Sweden; †Laboratory of Bioorganic Chemistry, National Institute of Chemical Physics and Biophysics, Tallinn, Estonia; and ‡Department of Theoretical Chemistry, Lund University, Chemical Centre, Lund, Sweden.

ABSTRACT Calmodulin (CaM) operates as a Ca^{2+} sensor and is known to interact with and regulate hundreds of proteins involved in a great many aspects of cellular function. It is of considerable interest to understand the balance of forces in complex formation of CaM with its target proteins. Here we have studied the importance of electrostatic interactions in the complex between CaM and a peptide derived from smooth-muscle myosin light-chain kinase by experimental methods and Monte Carlo simulations of electrostatic interactions. We show by Monte Carlo simulations that, in agreement with experimental data, the binding affinity between CaM and highly charged peptides is surprisingly insensitive to changes in the net charge of both the protein and peptide. We observe an increase in the binding affinity between oppositely charged partners with increasing salt concentration from zero to 100 mM, showing that formation of globular CaM-kinase type complexes is facilitated at physiological ionic strength. We conclude that ionic interactions in complex formation are optimized at pH and saline similar to the cell environment, which probably overrules the electrostatic repulsion between the negatively charged Ca^{2+}-binding domains of CaM. We propose a conceivable rationalization of CaM electrostatics associated with interdomain repulsion.

INTRODUCTION

The eukaryotic Ca^{2+} sensor calmodulin (CaM) is implicated in a large number of cellular processes. Over 100 CaM-regulated target proteins have been reported, including protein kinases, ion channels (1,2), and the inositol tris 1,4,5-phosphate receptor (3). A number of different ''structural modes of interaction'' with target protein have been identified (4), usually involving a helical segment in the target protein.

In complexes with kinases, $(Ca^{2+})_4$-CaM binds to a segment of the partner protein rich in positively charged and hydrophobic residues. An isolated 20-residue target sequence corresponding to residues 796–815 (1–20 in this work) in chicken gizzard smooth-muscle myosin light-chain kinase (smMLCKp or P7) retains its affinity for CaM and represents an adequate model for a complex of CaM with intact smMLCK protein (5). In the globular $(Ca^{2+})_4$-CaM-P7 complex the protein is wrapped around the α-helical peptide. All the lysine and arginine charges of P7 are in close contact with negatively charged side chains of acidic residues of CaM (6). In addition to paired ionic interactions in the complex, the net charges of unbound CaM and peptide are large and opposite. Accordingly, electrostatic interactions are expected to be importantly involved in formation of CaM complexes. However, they do not seem to be significantly manifested in binding affinity, which is highly surprising. For example, replacement of any positively charged residue by alanine in the CaM-binding sequence of MLCK from skeletal muscle does not result in decreased affinity, but rather an increase was observed (7). This unexpected observation was recently confirmed in another study (8). Even more intriguing results were obtained for complex formation between smMLCK peptides and CaM (9). The binding affinity was found to be essentially independent of changes in the net charge of peptide between +4 and +8, and of CaM from −6 to −18 (9). This observation was made while monitoring the binding equilibria in low-ionic-strength buffer where electrostatic interactions are supposed to be close to maximum. An analysis of the interaction of a protein with an oppositely charged surface shows that electrostatic interactions become ''saturated'' provided the surface is highly charged (10). The same type of ''saturation'' appears to take place in the case of CaM-target complex formation.

In this study we find an increase in binding affinity with added salt for highly and oppositely charged CaM and MLCK peptides. (See Table 1 for peptide nomenclature.) In many cases, the binding affinity for a charged ligand to an oppositely charged protein is reduced on salt addition or charge reduction, although the effect can be complicated by desolvation penalties. To shed some light on the unusual manifestation of electrostatic interactions in CaM action we investigated the combined effect of salt and pH on complex formation between CaM and MLCK peptides of variable charge number. Monte Carlo simulations of electrostatic interactions in the complex formation are performed along with experimental studies. We show that the complex formation at physiological ionic strength and pH still occurs in conditions of saturated electrostatic interactions. We find that despite the opposite charges of CaM and MLCK peptides the complex formation is facilitated by reduction of ionic interactions with added salt. We suggest that at low ionic strength the collapse of CaM into a globular complex

Submitted June 15, 2005, and accepted for publication December 22, 2005.
Address reprint requests to Sara Linse, Dept. of Biophysical Chemistry, Lund University, Chemical Centre, P.O. Box 124, Lund, Sweden. Tel.: 46-46-222-8238; Fax: 46-46-222-4543; E-mail: sara.linse@bpc.lu.se.

0006-3495/06/04/2903/08 $2.00
doi: 10.1529/biophysj.105.068718

TABLE 1 Peptide nomenclature

Peptide	charge	modifications
P7	+7	–
$P7_{ac\text{-}am}$	+7	ac, am
$P6_G$	+6	K7G
$P6_Q$	+6	K7Q
P5	+5	K7E
P4	+4	K4Q, K7Q, R17Q

All the peptides are derivatives of smMLCKp (P7), ARRKWQKTGHAVRAIGRLSS, with the modifications as indicated. ac, acetylated N-terminus; am, amidated C-terminus.

with smMLCK peptides might be disfavored by the repulsion between the negatively charged domains. The repulsion between CaM domains apparently becomes overridden by increasing ionic strength to near-physiological values, where the formation of a wrapped complex is facilitated.

MATERIALS AND METHODS

Chemicals, proteins, and peptides

All chemicals were of the highest grade. The expression and purification of CaM wild-type (wt) and mutants, as well as the synthesis and purification of peptide wt and variants, has been described earlier (9). P7 was also produced recombinantly in the IMPACT system (New England Biolabs, Beverly, MA) and purified according to the instructions by the manufacturer. N- and C-terminal domains of CaM (TR1C and TR2C, respectively, corresponding to residues 1–75 and 78–148, respectively, of CaM) were purified as previously described (11,12). Purity was confirmed by agarose and sodium dodecyl sulfate polyacrylamide gel electrophoresis as well as ^{1}H NMR. The concentrations were determined by absorbance at 280 nm (or 265 nm for TR1C) using an extinction coefficient of 3200 M^{-1} cm^{-1} for Ca^{2+}-CaM (13), 2950 M^{-1} cm^{-1} for TR1C, 760 M^{-1} cm^{-1} for TR2C, and 5550 M^{-1} cm^{-1} for each peptide (14), as confirmed by amino acid analysis after acid hydrolysis.

Fluorescence spectroscopy

Binding constants were obtained from titrations of peptide with protein in 5 mM buffer containing 1 mM $CaCl_2$ and NaCl concentrations ranging from 0 to 3 M. Sodium acetate, MES, Bis-Tris, Tris, Bis-Tris propane, Tricine, and CAPS were used as buffers to cover the pH range from 4 to 11. Overlapping buffering areas were used to test for specific buffer effects on the binding, but none were found. The pH readings taken before and after titration agreed within ±0.1 units. Below pH 5, the Ca^{2+} concentration was increased to 3–5 mM to saturate CaM. The peptide concentration was between 0.3 and 2 μM, and calmodulin aliquots were added from a concentrated stock solution. Fluorescence data were obtained with excitation at 295 nm and emission at 335 nm, as previously described (9). The reported binding constants are averages of at least two independent measurements, except for the CaM mutants, where an average is reported for all mutants binding to the same peptide and the error in binding constants is $<\pm 0.2$ log units. Fluorescence titration data were analyzed according to a 1:1 binding model, as previously described (9). In cases of weak binding, a large number of CaM titration points had to be collected and a linear part proportional to the concentration of unbound CaM was added to the fitting function. For binding between tryptic fragments and peptides, the stoichiometry of the formed complexes was an extra adjustable parameter in the fits. Binding constants above 10^8 M^{-1} are difficult to determine, prohibiting a comparison of different CaM charge mutants at high salt.

CD spectroscopy

CD spectra (180–250 nm, response time 16 s, resolution 1 nm, scan rate 20 nm/min, four scans averaged) were obtained at 5°C using a Jasco J-720 spectropolarimeter with a Jasco PTC-343 Peltier type thermostatic cell holder and a quartz cuvette with a path length of 1 mm. The peptide concentration was 46–74 μM at pH 7.2–7.3. smMLCKp adopts a random coil in solution at room temperature as shown by circular dichroism (CD) spectroscopy. To be able to compare the helix propensity and its salt dependence for the smMLCKp charge variants, the helical state needs to be favored. This was done by lowering the temperature to 5°C and by addition of trifluoroethanol (TFE) that shifts the coil to helix equilibrium toward the helical state. The helix propensity of different charge variants of smMLCKp was estimated from far-ultraviolet CD spectra in 20% TFE at 5°C, taking a CD signal at 221 nm of −35,300 deg cm^2 $dmol^{-1}$ (15) to represent a fully formed helix. The CD signal at 221 nm was converted into fraction helix for the different peptides in 20% TFE and the salt dependence of the helix formation was studied by adding 100 mM NaF. Difference spectra for complexes of P4 or P7 with CaM were generated by digitally subtracting the spectra of free CaM and free peptide from the spectra recorded for 1:1 complex of 10 μM peptide and 10 μM CaM in 5 mM Tris pH 7.5, as well as in 5 mM NaAc at pH 5.0. Data for substoichiometric mixtures were obtained by titrating P4 or P7 into 30 μM CaM in 5 mM Tris pH 7.5 and 5 mM NaAc at pH 5.0.

Isothermal calorimetry

The enthalpy associated with CaM-smMLCKp binding was determined by isothermal titration microcalorimetry using a VP-ITC instrument manufactured by Microcal (Northhampton, MA). Peptide stock (120–280 μM) was injected (5–11 μl per injection) into the 1.42-ml reaction cell containing 6–14 μM CaM or TR1C in 5 mM MOPS, pH 7.5, with 2 mM $CaCl_2$ and 0 or 100 mM NaCl. Controls included injection of peptide after complete saturation of CaM and injection of peptides into buffer. Wintrode and Privalov previously reported weak buffer dependence of smMLCKp binding to CaM at pH 7.0, so the measured heats should represent the intrinsic heat of binding. The data obtained from titration experiments were analyzed using the Origin software package for isothermal titration calorimetry (ITC) analysis from Microcal and Mathlab (Mathworks, Natick, MA). For most cases a 1:1 binding model was used to fit the data but for two peptides in low salt (P7 and P4) a second lower-affinity binding step was observed and then a sequential binding model was used to fit the data, and the reported enthalpy value is for the first binding step. The binding is too strong to allow determination of binding constants by ITC except for P4. For this peptide log K values of 7.5 and 7.0 were found in 5 mM buffer and in 100 mM NaCl, respectively. These values are in excellent agreement with those measured by fluorescence spectroscopy.

NMR relaxation measurements

The backbone dynamics of the complex of CaM and $P7_{am\text{-}ac}$ was studied by ^{15}N relaxation measurements in 0 and 100 mM KCl using ^{15}N-labeled protein. R_1, R_2, and $\{^1H\}$-^{15}N nuclear Overhauser effect (NOE) values were determined using previously published assignments for the complex (16). No peaks associated with free protein could be found, indicating that CaM was fully saturated with Ca^{2+} and peptide. Both Ca^{2+} and peptide dissociate from the complex slowly on the NMR timescale, so the dynamics of the components in the complex could be studied.

CaM and $P7_{am\text{-}ac}$ were dissolved in 1.4 ml ultrapure H_2O (Millipore, Bedford, MA, 0.22 μm) and the sample was concentrated and buffer exchanged using a Vivaspin concentrator. The final sample volume was 300 μl, containing 1 mM CaM, 1.2 mM peptide, 5 mM $CaCl_2$, 0.2 mM NaN_3, 0.1 mM DSS, 10% D_2O, and 0 or 100 mM KCl. The final pH values were 6.7 and 7.6, respectively, for the 0- and 100-mM samples. Spin-lattice (R_1) and spin-spin (R_2) relaxation rate constants, as well as $\{^1H\}$-^{15}N steady-state

hetero-NOEs were measured using two-dimensional pulse field gradient-enhanced experiments as described (17) using a 600-MHz Varian UNITY PLUS spectrometer operating at a ^{1}H frequency of 599.89 MHz. Spectra were acquired with 2048 complex points in $\omega 2$ (^{1}H), spectral width 7500 Hz, and 128 complex points in $\omega 1$ (^{15}N), spectral width 1800 Hz. The recovery times between experiments were 1.5 s, 2.0 s, and 10.0 s for R_1, R_2, and $\{^1H\}$-^{15}N, respectively. R_1 values were determined at 25°C with the following spectral delays: 2 (*2), 170, 320, 470 (*2), 620, 770 (*2), 920, 1220, 1370 (*2), and 1520 ms. R_2 values were determined at 25°C with the following spectral delays: 2 (*2), 4, 6 (*2), 8 (*2), 10, 120, 140, 180, 250, and 300 (*2) ms. (*2) indicates experiment duplicates. In the NOE experiment, two spectra were recorded interleaved, one with NOE and one without. All spectra were processed using the nmrpipe program suite with Lorentzian-to-Gaussian transformation in $\omega 2$ and a shifted sinebell in $\omega 1$. Relaxation rates were estimated by nonlinear fitting of an exponential function to the experimental data.

Computational details

The thermodynamic binding constant, K_{TH}, for a process where a protein (P) binds a ligand (L) and forms a complex (PL) can be formally written as

$$K_{TH} = \frac{a_{PL}}{a_P a_L} = \frac{C_{PL}}{C_P C_L}\frac{\gamma_{pL}}{\gamma_P \gamma_L}, \quad (1)$$

where a, C, and γ are activities, concentrations, and activity factors, respectively, for the molecules indicated by subscripts. In Eq. 1 we have also made use of the relation $a = \gamma C$. The first ratio on the right-hand side of Eq. 1 is the stoichiometric binding constant, $K_s = C_{PL}/C_P C_L$. This is the quantity measured in the experiments. Thus, since K_{TH} is a true constant, any measured change in K_s reflects a change in the activity factors. The activity factor is related to the excess chemical potential,

$$\mu_{ex} = kT \ln \gamma, \quad (2)$$

which is the quantity obtained from the Monte Carlo simulations. We will restrict ourselves to measured changes in the stoichiometric binding constant. Hence, from Eqs. 1 and 2, it follows that the ratio of two stoichiometric binding constants is given by

$$kT \ln\left(\frac{K_s^{II}}{K_s^{I}}\right) = kT\Delta \ln K_s = -\Delta\mu_{ex}^{B} + \Delta\mu_{ex}^{L}. \quad (3)$$

The notation ''I'' and ''II'' could, for example, correspond to the binding at two different pH values and $\Delta\mu = \mu(II) - \mu(I)$. The indices ''B'' and ''L'' stand for bound and free peptide, respectively. The excess chemical potentials in Eq. (3) are averaged over all protonation states of the protein.

The above equations are formally exact, but in the following text, the focus will be on electrostatic interactions only and we will assume that the change in binding constant is solely due to electrostatics. Note also that it is the shift in binding constant that is calculated. This means, for example, that structural changes upon binding do not affect the result as long as they are the same at different conditions. It also means that any ''self-energy terms'' cancel when the salt effect is studied; not necessarily because the self-energy of the bound and unbound form are the same but because the difference in self-energy between bound and unbound forms at two different salt levels are similar. The self-energy itself can be a large term.

We use a dielectric continuum model for the description of the protein solution. Thus, the atomic details of the solvent (water) are assumed to be of secondary importance and the water is characterized only by its dielectric permittivity, $\varepsilon_r = 78.3$, at room temperature. However, the protein atoms and the salt particles are treated explicitly as independent particles. Negatively charged amino acids, Glu, Asp, and the C-terminus, are given a charge of $-e$ divided equally between the two carboxylic oxygens. A positive unit charge is assigned to the appropriate nitrogen atoms of basic amino acid residues including Lys, Arg, His, and the N-terminus. All other protein atoms are treated as hard spheres with a radius of 2 Å—the same hard-core radius is assigned to charged protein atoms and any added positive and negative salt ions. With this model, the protein has a nonuniform charge distribution and the detailed form of the protein is taken into account using an experimentally determined structure for the protein-peptide complex (6).

We have assumed a uniform dielectric constant throughout the solution that is equal to the value for pure water. The interaction energy between any two particles can be formally described by

$$u(r_i, r_j) = \frac{q_i q_j e^2}{4\pi\varepsilon_r\varepsilon_0|\vec{r}_i - \vec{r}_j|}, \; r > \sigma \quad (4)$$

$$u(\vec{r}_i, \vec{r}_j) = \infty \; r < \sigma, \quad (5)$$

where e and ε_0 are the elementary charge and electric permittivity for vacuum, respectively, and $\sigma = 4$ Å. Hence, the total energy is a sum over all charged particles $U_{tot} = \sum_{i=1}\sum_{j>i} u(\vec{r}_i\vec{r}_j)$.

We use the standard Metropolis algorithm (18) and the protein atoms are kept fixed at the experimental x-ray coordinates, whereas counterions and salt particles are subject to moves in the Monte Carlo (MC) algorithm. In addition to the interactions described above, we have also introduced a confining sphere for the protein and the ions whose radius defines the protein concentration, which was set to 100 μM except for high ion strengths where a concentration of 800 μM was used. The ionization status of acidic and basic amino acid residues is in principle unknown and varies with pH, salt concentration, and protein concentration, as well as the binding of any ligand. This has been taken into account in the simulations by extending the canonical Metropolis algorithm to a semicanonical approach. Thus, the MC procedure consists of two types of moves: 1), random displacement of mobile salt particles; and 2), random change of the ionization status of titrating groups.

The acceptance of the second type of move is controlled by a change in electrostatic interactions plus the cost for ionizing/neutralizing the randomly chosen amino acid. The appropriate Boltzmann factor reads

$$\exp[-\Delta U_{tot}/kT \pm \ln 10(\mathrm{pH} - pK_a)], \quad (6)$$

where pK_a is the acid constant for the particular amino acid. After completion of this semicanonical MC scheme one obtains the average charge on each titrating residue and the net charge of the protein. The free energy of binding for the peptide is obtained from the MC simulations using a perturbation technique (19,20). Both the excess chemical potential of the bound and free peptide are obtained from the same simulation. In the first case, the peptide is inserted in the binding site, whereas in the latter the peptide is inserted at random in the MC sphere. The excess chemical potential is then obtained as a canonical average,

$$\mu_{ex} = -\mathrm{kT} \ln < \exp(-U_{test}(\vec{r})/\mathrm{kT}) >_0, \quad (7)$$

where $U_{test}(\vec{r})$ is the interaction energy between a peptide inserted at position $\vec{r}$ and all other particles. The brackets denote an ensemble average over the unperturbed system. The accuracy of the calculated μ_{ex} for an octavalent peptide is of the order of a few tenths of a kT.

RESULTS AND DISCUSSION

pH-dependent peptide binding to CaM

For the oppositely charged CaM and P7, it seems reasonable to expect that the binding affinity is sensitive to changes in pH that modulate the charges of the protein and peptide. As seen in Fig. 1, the effect of pH is widespread and affects the average charge of a large number of titrating residues in the protein, as well as the histidine residue of the peptide. However, complex formation between CaM and P7 turned out to

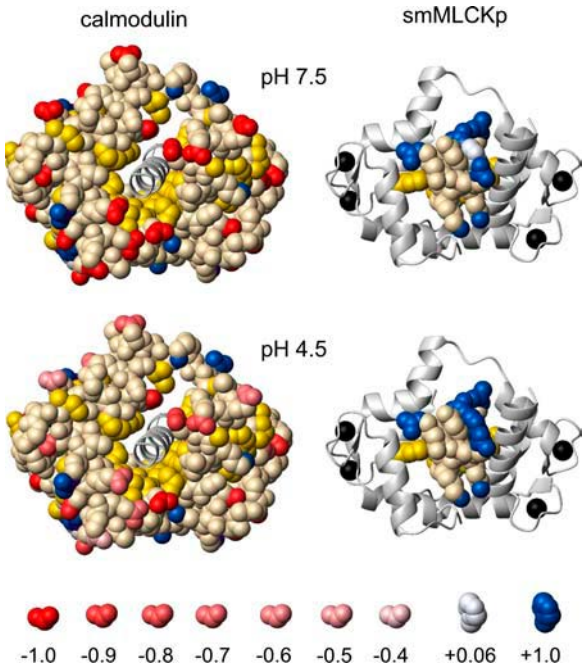

FIGURE 1 Three-dimensional structure of the calmodulin-P7 complex (PDB code 1cdl (6)) shown as space-filling models with hydrophobic, acidic, and basic side chains in yellow, red, and blue, respectively. The average net charge of each residue at pH 7.5 and pH 4.5 is shown separately for each component with the other component as ribbons.

be virtually independent of large changes in the net charge in the pH range from 5 to 11 in a low-ionic-strength buffer (9). Because of the long-range nature of electrostatic interactions, changes in the charge state of the protein affect the peptide as much in its free as in its bound state, leading to a virtual pH independence of binding over a wide range of pH values. At pH values close to the isoelectric point, an additional cause of the diminished response of binding affinity to changes in pH is a charge regulation mechanism. In particular, highly charged biopolymers change their net charge in response to one another by releasing or binding protons at ionizable residues (21). One might expect that increasing the salt concentration makes the binding even less sensitive to changes in pH. In contrast, we find that the pH dependence of CaM-peptide complex formation in 1 M NaCl is more pronounced than in the absence of NaCl (Fig. 2). In 1 M NaCl, the log K values show a bell-shaped pH dependence with a maximum around pH 8. Between pH 4.5 and pH 8 we see an increase in binding affinity by 1.5 log K units. A further increase in pH leads to a decrease in binding constant, which could be due to structural changes in CaM and peptide.

A striking result is that in a wide range of pH values an increase in affinity is observed with added salt. The system thus behaves qualitatively as would be expected for an interaction between charged particles with the same sign.

The simulated pH dependence of binding in 761 mM salt is shown in Fig. 2. Here the addition of salt has no effect on the binding in the pH range between 5 and 9, and this

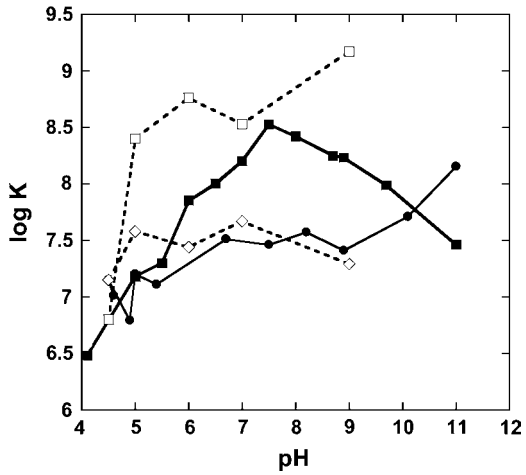

FIGURE 2 Experimental pH dependence of log K as a function of pH for binding of P7 to CaM in 5 mM buffer (*solid line* with *solid circles*) (data from André et al. (9)) and in 1 M NaCl (*solid line* with *solid squares*). Simulated pH dependence of binding of $P7_{am\text{-}ac}$ in 1 mM (*dotted line* with *open diamonds*) and 761 mM (*dotted line* with *open squares*) salt.

behavior is a consequence of the high charge of the system. Instead of the log K optimum around pH 7.5 as found by experiment in 1 M salt, the simulations yield a plateau from pH 5 to pH 9. The reason for this discrepancy may be that the conformational changes that take place upon binding are dependent on pH and salt.

Salt dependence of peptide binding

Complex formation between oppositely charged molecules is usually facilitated by attractive electrostatic forces. Addition of electrolytes reduces the binding affinity due to screening of electrostatic interactions, e.g., as observed for the calcium binding to EF-hand sites of calbindin D_{9k} (22). An increase in binding affinity with added salt is expected when complex formation includes interaction between charges of the same sign. For the oppositely charged CaM and P7, it seems reasonable to expect that the addition of salt reduces the binding constant (in the neutral pH region). The bell-shaped pH dependence at high salt (Fig. 2), however, shows that between pH 5.5 and pH 10 the calmodulin-target peptide interaction is enhanced at high salt. This calls for more detailed investigation of the salt dependence. The affinity between charge variants of CaM and the smMLCK peptide was previously determined at pH 7.5 in low-ionic-strength conditions. Here we have measured the binding constants in 100 mM KCl at pH 7.5 for all combinations of five CaM (wt, E84Q, E83Q, E14Q, and D78N) and four peptide ($P6_G$, $P6_Q$, P5, and P4) charge variants. The binding of wt CaM to $P7_{am\text{-}ac}$ was also studied. The results (Table 2) clearly show that the affinity for CaM increases with increasing ionic strength from 0 to 100 mM for all peptides except P4. It is also clear that for all CaM mutants, binding of the highly charged peptides (P5–P7) is tighter at 100 mM KCl than at low salt.

TABLE 2 Experimental equilibrium constant for binding of smMLCKp charge variants to wt CaM and its mutant forms with negative charge deletions

Protein	P7	$P6_Q$	$P6_G$	P5	P4	$P7_{am\text{-}ac}$ (0 mM NaCl)
CaM	8.4	8.0	8.5	8.0	7.1	7.6
E84Q	8.3	8.1	9.1	7.8	7.5	7.4
E83Q	8.6	8.5	9.5	8.1	7.2	7.4
E14Q	8.5	8.1	9.1	8.4	7.1	7.5
D78N	8.5	8.6	8.5	8.3	7.2	7.5
Average	8.5	8.3	8.9	8.1	7.2	7.5

All experiments were performed in 5 mM Tris and 100 mM KCl at pH 7.5 and 25°C. As a reference, the previously reported values for the binding of $P7_{am\text{-}ac}$ in 5 mM tris is included (9). The experimental equilibrium constant is expressed as $\log K = {}^{10}\log K$. The $\log K$ values are determined within ± 0.2 (± 0.3 for $P6_G$).

The positive salt effect is manifested as if the observed complex formation takes place in conditions of repulsive electrostatic interactions between the charged particles of similar sign. In the presence of 100 mM KCl, similarly increased binding affinities are observed for all the smMLCK peptide derivatives with variable net charge, but also for the mutant forms of CaM (Table 2). An exception is the derivative P4 with the lowest charge of +4, which shows a significantly reduced affinity for CaM and all the studied mutant forms (Table 2).

For P7, $P7_{am\text{-}ac}$, and P4, the binding to wt CaM was followed as a function of salt (Figs. 3 *a* and 4). P7 and $P7_{am\text{-}ac}$ both show an increased binding constant up to ~100 mM NaCl, after which a plateau is reached that extends up to 3 M NaCl for P7. Thus, in conflict with the naive picture, the affinity of the highly charged peptides for the oppositely charged protein increases with increasing salt concentration in the range 0–100 mM NaCl, after which no further increase is seen.

In contrast to the more highly charged peptides, for P4 the CaM-binding constant decreases with increasing concentrations of NaCl up to 0.5 M NaCl. Between 0.5 and 3 M NaCl there is then an increase in the binding constant. The origin of this increase should be primarily nonelectrostatic and could potentially be attributed to the salt dependence of hydrophobic interactions. The salt dependence of P4 binding hence shows a qualitatively expected behavior—a decrease in affinity with the addition of salt. The decrease is more pronounced at pH 5, where the system is not as highly charged compared to pH 7.5. So the lower charge of the system at pH 5 leads to stronger salt dependence. The results from the simulations agree with experiment in that a peptide with low charge is needed to obtain a ''normal'' salt dependence, i.e., decreased affinity with increasing salt concentration (Fig. 4). The simulation also predicts the more pronounced salt dependence at lower pH (Fig. 4). For the highly charged peptides, a weak salt dependence between 0 and 100 mM is predicted, in fair agreement with experiments (Fig. 3). However, the experimental increase in affinity as observed between 0 and 100 mM NaCl is not seen in simulations. The simulated salt dependence is larger at low than at high pH, where the protein is less charged, again indicating that electrostatic interactions take place under ''saturating'' conditions (Fig. 3).

TABLE 3 Experimental binding enthalpies in 0 and 100 mM NaCl

Peptide	charge	ΔH in 0 mM NaCl (kJ/mol)	ΔH in 100 mM NaCl (kJ/mol)	$\Delta\Delta H$ *(kJ/mol)*
P7	+7	−92	−63	29
$P6_G$	+6	−88	−69	19
$P6_Q$	+6	−103	−86	17
P5	+5	−103	−87	16
P4	+3	−105	−46	59

Binding enthalpies were measured in 5 mM MOPS at pH 7.5 and 25°C. ΔH values are determined with an accuracy of ±5%. $\Delta\Delta H$ values are defined as the difference in enthalpy between 100 and 0 mM NaCl.

TABLE 4 Fraction helix of smMLCKp charge variants in 20% TFE at 5°C

Peptide	Fraction helix (%) 0 mM NaF	Fraction helix (%) 100 mM NaF	$\Delta\Delta G$ (kJ/mol)
P7	4.0	4.7	−0.3
$P6_Q$	5.6	8.3	−1.0
P5	8.1	12.4	−1.1
P4	0.4	0.47	−0.4

The values indicate the free energy difference in coil-to-helix transition after the addition of 100 mM NaF, $\Delta\Delta G$ values are determined within ±0.2 kJ/mol.

The results of difference CD spectroscopy show that the peptide is bound in the same helical conformation, regardless of net charge or pH. Difference CD spectra of P4 or P7 bound to CaM compared to free components show that the same amount of helicity is induced in P4 and P7 upon binding at pH 7.5, indicating that P4 is also fully helical in the complex. Also both peptides show the same capacity to adopt a helix on complex formation at pH 5.0 and 7.5. ^1H-^{15}N heteronuclear single quantum coherence spectra of $P7_{am\text{-}ac}$-CaM complex in low and 100 mM KCl does not provide any evidence of large conformational changes with the addition of salt (data not shown).

Although the simulations capture many essential features of the experimental results (larger pH sensitivity at high compared to low salt, and more ''normal'' salt dependence in a system with lower charge), the agreement is not perfect and the increase in affinity with added salt for the highly charged system is not seen in simulations. However, the agreement is much better than what is achieved using the popular Debye-Hückel approximation. A traditional and often useful way to calculate the same quantities as we have done here in the Monte Carlo simulations is to use the so-called Tanford-Kirkwood model. This takes into account the detailed charge distribution of both peptide and protein, and the complex. The electrostatic interactions are, however, calculated only within the Debye-Hückel approximation, which is not a valid approach considering the high charge on both calmodulin and the peptides (23). The Tanford-Kirkwood

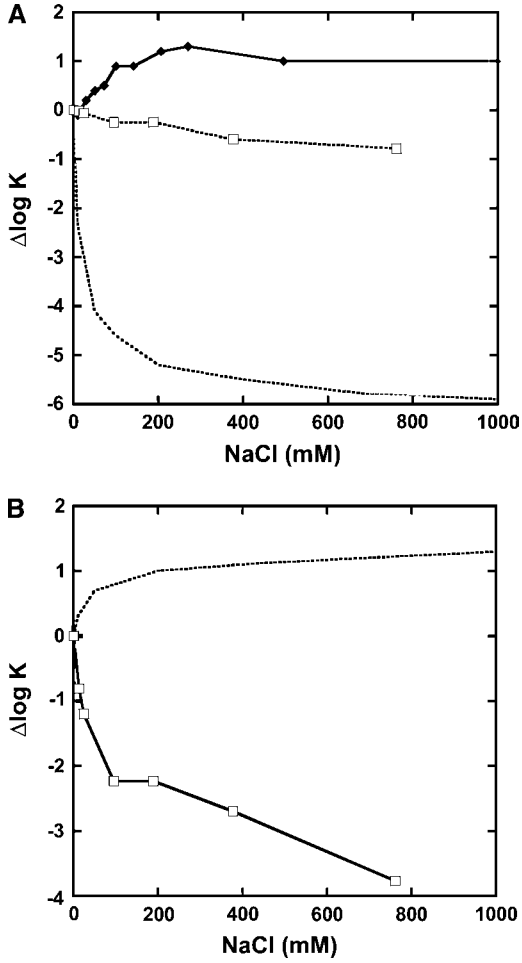

FIGURE 3 (*a*) Experimental salt dependence of log K as a function of concentration of NaCl for P7 (*solid line* with *diamonds*). Simulated salt dependence of binding for the $P7_{am\text{-}ac}$ to CaM, averages for pH values in the range 6–9 using MC (*dotted line* with *open squares*) and at pH 7.5 using Tanford-Kirkwood (*dotted line*). (*b*) Simulated salt dependence of binding for $P7_{am\text{-}ac}$ to CaM, averages for pH values in the range 3.5–5.5 using MC (*solid line* with *open squares*) and at pH 4.5 using Tanford-Kirkwood (*dotted line*).

model predicts that the binding constant increases as a function of salt at low pH and that it decreases as a function of salt at high pH. It also predicts a much too large shift upon change of pH, both at low and high salt concentration.

The failure of the Tanford-Kirkwood theory at low pH is due to the neglect of charge regulation. That is, when a positively charged peptide binds to a protein there will be a release of protons from acidic residues. This mechanism is included in the simulations, whereas the Tanford-Kirkwood model assumes a fixed charge distribution equal to that of the unperturbed protein. At high pH, Tanford-Kirkwood overestimates the salt response due to the underlying linearization approximation, and the simulated curve is closer to experiment. However, both theoretical approaches neglect structural changes in CaM, and this is probably the main reason for the difference between Monte Carlo simulation results and experiments.

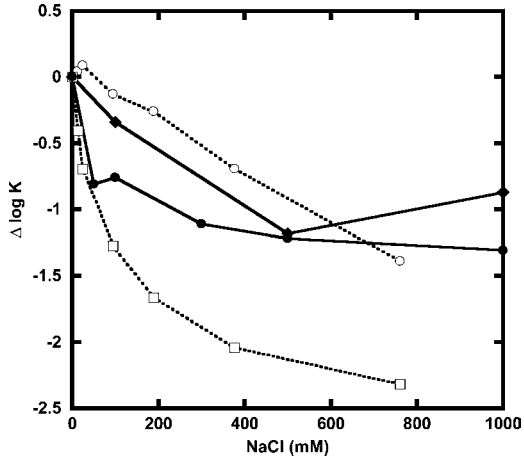

FIGURE 4 Experimental salt dependence of log K as a function of concentration of NaCl for P4 binding to CaM at pH 7.5 (*line* with *solid diamonds*) and P4 binding to CaM at pH 5 (*line* with *solid circles*). Simulated salt dependence of binding of P4 to CaM, averages for pH values in the ranges 3.5–4.5 (*dotted line* with *open squares*) and 6–9 (*dotted line* with *open circles*).

Salt effect on the binding of $P7_{am\text{-}ac}$ to tryptic fragments of CaM, TR1C, and TR2C shows a decrease in binding affinity with increasing salt concentration, as usually observed for complex formation between oppositely charged molecules (Fig. 5). For TR2C, the obtained stoichiometry is close to one fragment per peptide up to 100 mM NaCl but increases to 1.6 at 1 M NaCl. For TR1C, we observe a change in stoichiometry from one fragment per peptide at low salt, between one and two at 100 mM NaCl, and up to around four TR1C per peptide at 1 M salt. NMR self-diffusion measurements of 1:1 mixtures of TR1C and $P7_{am\text{-}ac}$ in 0–200 mM NaCl also indicate a complex salt dependence for the stoichiometry (data not shown). Despite these complications, it is clear that both TR1C and TR2C show the expected salt dependence with decreased peptide-binding affinity up to 1 M NaCl. At low salt, the binding affinity of $P7_{am\text{-}ac}$ for TR1C and TR2C is similar to the binding affinity of $P7_{am\text{-}ac}$ for intact CaM (log $K = 7.5$ for TR1C, 7.9 for TR2C, and 7.6 for CaM). Hence, at low salt the presence of a second domain as in intact CaM does not contribute much to the binding affinity. However, around physiological salt, CaM is a much more potent peptide binder than any one of the isolated domains. For example, at 100 mM NaCl, the peptide-binding affinity is 40- to 70-fold higher for calmodulin compared to TR1C and TR2C. This shows that salt screening allows the two domains to cooperate in binding and chelate the peptide more tightly.

The salt dependence of binding shows that only when the charge of the system is reduced via either protein or peptide will the system behave qualitatively as expected and predicted by simulation. Again this indicates that pH and salt affect the conformational changes that occur upon complex formation.

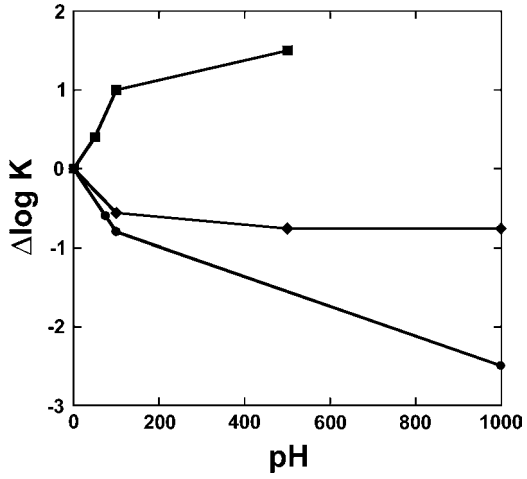

FIGURE 5 Experimental salt dependence of log K as a function of concentration of NaCl for $P7_{am\text{-}ac}$ binding to CaM (*squares*), TR1C (*diamonds*), and TR2C (*circles*) at pH 7.5.

Helix propensity

The process of binding a peptide to CaM may be divided into coil-to-helix transition and binding of the helical peptide to CaM. Addition of salt expected to reduce the electrostatic penalty of forming a helix with a large number of like charges. Indeed, our CD measurements show an increased helical signal for all peptides upon addition of 100 mM NaF (Table 4). This corresponds to a decrease in the free energy of helix formation of 0.3–1.1 kJ/mol, accounting for 5–20% of the salt-induced decrease in free energy of binding.

Backbone dynamics of the $P7_{am\text{-}ac}$-CaM complex

An NMR relaxation study was performed to address the compactness of the calmodulin-peptide complex at low and high salt. The R_2, but not R_1 or NOE, data show a significant difference in backbone dynamics between low and 100 mM NaCl. The R_1/R_2 ratio is on average 8% lower for the complex in 100 mM compared to low salt (data not shown). This can be interpreted in terms of an increased rotational correlation time of the complex.

Calorimetric data

For all measured peptides the enthalpy of binding to CaM increases with the addition of 100 mM NaCl (Table 3). P4 has a significantly larger increase in binding than the other peptides. Also, the enthalpy of binding P7 to TR1C is higher at 100 mM NaCl (−34.4 kJ/mol) than at 0 mM NaCl (−43.2 kJ/mol), and the apparent stoichiometry of TR1C to peptide increases with the addition of salt. The increase in enthalpy with salt is opposite to what should be expected from Debye-Hückel-type theory.

Binding of smMLCKp to CaM is an enthalpy-driven process associated with negative binding entropy (24). An increase in log K with salt means that the free energy of binding decreases, and since the enthalpy of binding increases, the free energy decrease must be a consequence of entropic factors. This is true for P4 also, where the increase in enthalpy with salt is significantly larger than the increase in free energy. The coil-to-helix transition of the peptide upon binding reduces the entropy of the system, and salt effects on the free peptides may account for a maximum of 20% of the observed free energy change. Other entropic factors involve the N- and C-terminal domains, which are moving independently in free CaM, and experience a loss in the number of available conformations upon peptide binding. Side-chains and backbone can have salt-dependent conformational entropy. The NMR relaxation data give no evidence for changes in backbone flexibility of CaM on the picosecond to nanosecond timescales. Finally, interactions between opposite charges and burial of hydrophobic surfaces in the complex increase the entropy of water.

Interdomain repulsion as a conceivable rationalization of CaM electrostatics

The anomalous salt dependence of the CaM-peptide interaction may be due to electrostatic repulsion between the two domains of CaM, both of which are highly negatively charged. At neutral pH, CaM has a formal net charge of −24 that is reduced to −16 upon Ca^{2+} binding, with the charges distributed between the N- and C-terminal domains. Several structures of CaM-target-peptide complexes show a peptide bound to the C-terminal lobe of extended CaM, leaving the N-terminal domain unbound. This is consistent with a higher net charge of the C-terminal than the N-terminal domain (−14 for TR2C and −10 for TR1C), indicating that basic peptides preferentially bind to the C-terminal domain. Salt dependence of peptide binding is more pronounced for TR2C than for TR1C, indicating a larger electrostatic component to the binding of peptide to the C-terminal domain. Even with peptide bound to the C-terminal domain, there remains a net negative charge on the domains. One may therefore imagine that the two domains are on average found at larger separation at low salt. Upon addition of salt the repulsive electrostatic interactions are screened and the two domains come closer together with a resulting gain in attractive van der Waal's interactions within the complex (Fig. 6). The model presented here relies on a conformational freedom of the two domains. If the peptide would bind to a static structure, the screening of intraprotein electrostatic interactions by salt would not affect the binding in the manner found in this work.

There are a number of experimental findings that are reconciled with this model. The affinity of binding of highly charged peptides to CaM is increased with addition of salt, a behavior normally seen in repulsive systems. For the tryptic fragments of CaM, salt addition leads to a decrease in peptide-binding affinity, indicating that in intact CaM the

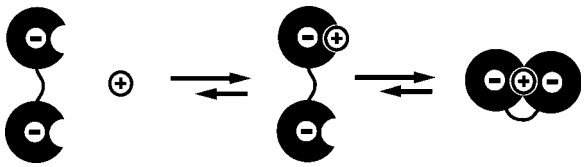

FIGURE 6 Domain repulsion model.

interactions between the domains are responsible for the unexpected increase in binding with salt. At low salt the binding of peptide to CaM is not stronger than the binding of peptide to the tryptic fragments, showing that the binding of an extra domain of CaM to the peptide does not lead to an increased binding affinity. In apo CaM, where more repulsion between the domains is expected due to the higher negative charge on CaM, peptides only bind to the C-terminal domain. For peptide binding to TR1C there is an apparent change in stoichiometry of binding with addition of salt, with an increased number of protein fragments bound per peptide at higher salt concentrations. This shows that repulsive interactions between the two domains can be overcome by screening of salt. Finally, higher R_2 relaxation rate values in low ionic strength is consistent with a fraction of peptides bound only to one domain since free CaM has shorter correlation times than the complex.

CONCLUSIONS

1. The binding of the highly charged smMLCKp to CaM is optimal at salt and pH conditions reminiscent of the conditions in the cell.
2. Complex formation between CaM and highly charged peptides takes place at ''saturating'' electrostatic interactions. That is, the binding affinity is remarkably invariant to large changes in the net charges of CaM and peptide.
3. The increase in affinity with added salt is due to entropic factors.
4. The facilitated formation of globular CaM-kinase-type complexes at physiological ionic strength is likely due to overruled electrostatic repulsion between the negatively charged Ca^{2+}-binding domains of CaM.

This work was supported by the Swedish Natural Science Foundation (I.A., B.J., and S.L.), and by the Estonian Science Foundation (T.K.)

REFERENCES

1. Gu, C., and D. M. Cooper. 1999. Calmodulin-binding sites on adenylyl cyclase type VIII. *J. Biol. Chem.* 274:8012–8021.
2. Lee, A., S. T. Wong, D. Gallagher, B. Li, D. R. Storm, T. Scheuer, and W. A. Catterall. 1999. Ca2+/calmodulin binds to and modulates P/Q-type calcium channels. *Nature.* 399:155–159.
3. Missiaen, L., J. B. Parys, A. F. Weidema, H. Sipma, S. Vanlingen, P. De Smet, G. Callewaert, and H. De Smedt. 1999. The bell-shaped Ca^{2+} dependence of the inositol 1,4, 5-trisphosphate-induced Ca^{2+} release is modulated by Ca^{2+}/calmodulin. *J. Biol. Chem.* 274:13748–13751.
4. Hoeflich, K. P., and M. Ikura. 2002. Calmodulin in action: diversity in target recognition and activation mechanisms. *Cell.* 108:739–742.
5. Kranz, J. K., E. K. Lee, A. C. Nairn, and A. J. Wand. 2002. A direct test of the reductionist approach to structural studies of calmodulin activity: relevance of peptide models of target proteins. *J. Biol. Chem.* 277:16351–16354.
6. Meador, W. E., A. R. Means, and F. A. Quiocho. 1992. Target enzyme recognition by calmodulin: 2.4 Å structure of a calmodulin-peptide complex. *Science.* 257:1251–1255.
7. Montigiani, S., G. Neri, P. Neri, and D. Neri. 1996. Alanine substitutions in calmodulin-binding peptides result in unexpected affinity enhancement. *J. Mol. Biol.* 258:6–13.
8. Hultschig, C., H. J. Hecht, and R. Frank. 2004. Systematic delineation of a calmodulin peptide interaction. *J. Mol. Biol.* 343:559–568.
9. Andre, I., T. Kesvatera, B. Jönsson, K. S. Åkerfeldt, and S. Linse. 2004. The role of electrostatic interactions in calmodulin-peptide complex formation. *Biophys. J.* 87:1929–1938.
10. Engström, S., and H. Wennerström. 1978. Ion condensation on planar surfaces—solution of Poisson-Boltzmann equation for 2 parallel charged plates. *J. Phys. Chem.* 82:2711–2714.
11. Finn, B. E., J. Evenäs, T. Drakenberg, J. P. Waltho, E. Thulin, and S. Forsen. 1995. Calcium-induced structural changes and domain autonomy in calmodulin. *Nat. Struct. Biol.* 2:777–783.
12. Bentrop, D., I. Bertini, M. A. Cremonini, S. Forsen, C. Luchinat, and A. Malmendal. 1997. Solution structure of the paramagnetic complex of the N-terminal domain of calmodulin with two Ce3+ ions by 1H NMR. *Biochemistry.* 36:11605–11618.
13. Klee, C. B. 1977. Conformational transition accompanying the binding of Ca2+ to the protein activator of 3′,5′-cyclic adenosine monophosphate phosphodiesterase. *Biochemistry.* 16:1017–1024.
14. Pace, C. N., F. Vajdos, L. Fee, G. Grimsley, and T. Gray. 1995. How to measure and predict the molar absorption coefficient of a protein. *Protein Sci.* 4:2411–2423.
15. Scholtz, J. M., H. Qian, E. J. York, J. M. Stewart, and R. L. Baldwin. 1991. Parameters of helix-coil transition theory for alanine-based peptides of varying chain lengths in water. *Biopolymers.* 31:1463–1470.
16. Roth, S. M., D. M. Schneider, L. A. Strobel, M. F. Van Berkum, A. R. Means, and A. J. Wand. 1992. Characterization of the secondary structure of calmodulin in complex with a calmodulin-binding domain peptide. *Biochemistry.* 31:1443–1451.
17. Farrow, N. A., R. Muhandiram, A. U. Singer, S. M. Pascal, C. M. Kay, G. Gish, S. E. Shoelson, T. Pawson, J. D. Forman-Kay, and L. E. Kay. 1994. Backbone dynamics of a free and phosphopeptide-complexed Src homology 2 domain studied by 15N NMR relaxation. *Biochemistry.* 33:5984–6003.
18. Metropolis, N., A. W. Rosenbluth, M. N. Rosenbluth, A. H. Teller, and E. Teller. 1953. Equation of state calculations by fast computing machines. *J. Chem. Phys.* 21:1087–1092.
19. Svensson, B. R., and C. E. Woodward. 1988. Widom method for uniform and non-uniform electrolyte solutions. *Mol. Phys.* 64:247–259.
20. Widom, B. 1963. Some topics in theory of fluids. *J. Chem. Phys.* 39: 2808–2812.
21. Lund, M., and B. Jönsson. 2005. On the charge regulation of proteins. *Biochemistry.* 44:5722–5727.
22. Kesvatera, T., B. Jönsson, E. Thulin, and S. Linse. 1994. Binding of Ca2+ to calbindin D9k: structural stability and function at high salt concentration. *Biochemistry.* 33:14170–14176.
23. Da Silva, F. L., B. Jönsson, and R. Penfold. 2001. A critical investigation of the Tanford-Kirkwood scheme by means of Monte Carlo simulations. *Protein Sci.* 10:1415–1425.
24. Wintrode, P. L., and P. L. Privalov. 1997. Energetics of target peptide recognition by calmodulin: a calorimetric study. *J. Mol. Biol.* 266: 1050–1062.